

Review

# A Brief Overview on the Anticorrosion Performances of Sol-Gel Zeolite Coatings

Luigi Calabrese \* and Edoardo Proverbio

Department of Engineering, University of Messina, Contrada di Dio Sant'Agata, 98166 Messina, Italy; eproverbio@unime.it

\* Correspondence: lcalabrese@unime.it; Tel.: +39-090-676-5544

Received: 24 May 2019; Accepted: 20 June 2019; Published: 24 June 2019



**Abstract:** Research activity concerning nanoporous zeolites has grown considerably in recent decades. The structural porosity of zeolites provides versatile functional properties such as molecular selectivity, ion and molecule storage capacity, high surface area, and pore volume which combined with excellent thermal and chemical stability can extend its application fields in several industrial sectors. In such a context, anti-corrosion zeolite coatings are an emerging technology able to offer a reliable high performing and environmental friendly alternative to conventional chromate-based protective coatings. In this article, a focused overview on anti-corrosion performances of sol-gel composite zeolite coatings is provided. The topic of this review is addressed to assess the barrier and self-healing properties of composite zeolite coating. Based on results available in the literature, a property–structure relationship of this class of composites is proposed summarizing, furthermore, the competing anti-corrosion active and passive protective mechanisms involved during coating degradation. Eventually, a brief summary and a future trend evaluation is also reported.

**Keywords:** coatings; corrosion; zeolite; functional coatings; sol-gel

---

## 1. Introduction

One of the widely used cost-effective methods for corrosion protection of metallic substrates is to apply surface engineering coatings [1]. In recent years, the research and development of environmentally friendly alternatives to chromate based coatings, due to their high toxic and carcinogenic limits, was widely investigated [2]. In this context, several developments have been made in the use of composite coatings that offer a synergistic action of active inhibition and corrosion barrier [3].

The barrier properties of a coating can slow down the diffusion rate of the aggressive electrolyte towards the metal substrate. However, the presence of local defects or damage on the coating surface may allow an easier penetration of the aggressive species towards the metal interface, strongly limiting its durability [4]. Consequently, the synergistic integration of the barrier action with active protection—e.g., through the addition of green inhibitors—represents an effective and reliable potential development strategy to obtain longtime durable coatings [5,6].

Several classes of inhibitors were assessed in order to obtain chromate free and environmental friendly active coatings. In such a context, transition and rare earth metals ions demonstrated a multi-functional corrosion protection action acting effectively to inhibit localized corrosion phenomena in ferrous and non-ferrous alloys [7,8]. However, the approach to introduce the inhibitory species within the coating matrix, although simple and cost-effective, is not an efficient solution due to the required high content of the species and the possible interaction with the film matrix that leads to an immediate or progressive loss of its barrier effect over time [9]. Often, the corrosion inhibitors added to the coating suffers of undesirable rapid leakage which leads to its fast decrease over time, depleting its

potential effective self-healing action [10]. Furthermore, the usage of the corrosion inhibitor involves the presence of a zone of discontinuity, where it is entrapped in the cross-linked structure of the coating that act as hosting material, which can significantly damage its integrity [11].

In order to limit such issues, an alternative strategy is to inoculate the inhibitor inside a micro-nano-carriers obtaining a composite filler constituted by an inert reservoir activated by an inhibitory species placed inside it [12–14]. Indeed, in literature the use of inhibitors containers was investigated in order to offer a suitable mechanical and structural stability of the coating optimizing the interaction with the hosting matrix and, at the same time, to control the inhibitor release during time offering a selective self-healing action only in real corroding conditions [15]. Several micro- and nano-capsules were proposed in order to host green inhibitors for corrosion protection of coatings, including bentonite [16], montmorillonite [17], hydroxyapatites [18], carbon, or alloysite nanotubes [19]. For example, this approach applied on clay nano-containers filled with Ce (III) ions provides significant corrosion inhibition and ability to delay cathodic delamination; the effect being superior to that of chromate-based coatings [3].

The role of doped inorganic inhibitors in the active anti-corrosion performances of coatings was also assessed by using mesoporous particles [20,21]. Fu et al. proposed hollow mesoporous silica nanoparticles as reservoir for smart coatings for aluminum substrate evidencing an effective delay of electrolyte penetration but mainly a self-repairing action on damaged areas of the coating. Analogously, Hollamby [22] proposed a mesoporous silica nanoparticles doped with benzotriazole as smart filler for a polyester primer. They evidenced that this approach can be used to design reliable and durable hybrid functional coatings.

However, the morphology and the micro- and meso-porosity of the capsule play an important role in the design of an effective inhibiting nano-container suitable for corrosion protection [23]. In order to tailor the micro-nano-containers, some features need to be guaranteed, such as (i) chemical and mechanical stability, (ii) chemical compatibility with the coating matrix, (iii) effective loading capacity, (iv) to limit accidental inhibitor release, (v) corrosion selectivity, and (vi) on-demand release of the hosted inhibitor [24]. In such a context, a really promising approach that in the last year was acquiring significant relevance and that allows a potentially reliable coating design, is the use of zeolite as filler and micro-container for inhibitor species encapsulation [25] favoring self-healing mechanisms in this class of new smart coatings [26,27]. More recently, Calabrese in [25] assessed the effectiveness and affordability to corrosion protection of pure zeolite coating, highlighting its promising capabilities.

Comparatively, aim of this article is to provide an overview on the anti-corrosion performances of composite zeolite filled coatings. The article, after a brief introduction on the microstructure and properties of the zeolite materials, draws a concise historical overview and outlines the new trends of zeolite composite coating technology related to the anti-corrosion topic. In particular, two subset sections have been detailed: thermosetting polymer paints and dip-coating zeolite composite coatings. Afterward, a specific section of the article is focused on property to structure relationships in composite zeolite coatings relating these aspects to the corrosion protection efficiency of the coating themselves.

Eventually, a last section was addressed on active and barrier anti-corrosion mechanisms of zeolite coatings assessing the active contribute of micro-porous structure of the zeolite on the development of active functional coatings. The final purpose is to give, on the basis of an overview of the state of the art in such a context, a rational and structured reference focused on innovations and development perspectives of this coating technology, highlighting, furthermore, the limits and the issues related to its usage in industrial applications.

## 2. Zeolites: Microstructure and Properties

Zeolites are micro-porous crystalline aluminosilicate crystals. Their structure is constituted by an array of  $\text{SiO}_4^{4-}$  or  $\text{AlO}_4^{5-}$  tetrahedron. The centers of tetrahedrons are by silicon or aluminum atoms and vertex by oxygen atoms, which act as a bridge between adjacent tetrahedrons. The building blocks become arranged in a three-dimensional structure characterized by channels and cavities obtaining a

crystal with very large specific surface area (typically about  $300 \text{ m}^2 \text{ g}^{-1}$  with the volume of internal voids about  $0.1 \text{ cm}^3 \text{ g}^{-1}$ ) [28].

In Figure 1, the tridimensional structure of a zeolite Y, selected as an example, is schemed. The zeolite structure consists of regular, intercommunicating cages and channels (dimension in the range 3–10 Å) resulting in a high surface area and large internal volume. Zeolite Y has two types of cages: sodalite cage and supercage. This latter is the largest cavity in the framework structure and it has an internal dimension of 7.4 Å. These cavities are usually occupied by water molecules or extra-reticular ions, but they are large enough to host guest species. These ions or molecules are not structural components of the aluminosilicate framework and can be respectively, exchanged, or removed without modification of the zeolite structure.

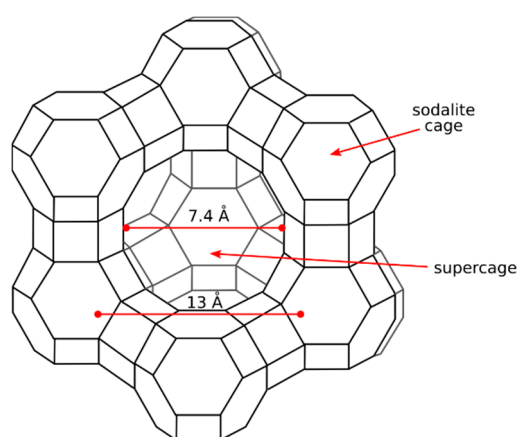


**Figure 1.** Scheme of the structure of zeolite Y.

The zeolites consequently possess a regular shaped micro-porosity, with molecular dimension, which makes the zeolite of fundamental importance and widely used in the chemical industry for adsorbent, catalytic, or ion exchange processes [2]. Although their main application is as a catalyst in the oil and petrochemical sector, they are used in other industrial sectors (e.g., agriculture, detergents, water treatment) [29–31], as well as a molecular sieve in separation membranes [32].

Additional interesting applications fields were investigated in literature, in order to extend its applicability in new industrial sectors ranging from dielectric [33,34] to antimicrobial [35–37] or adsorption heat pumps [38,39]. A large class of natural or synthetic zeolites (i.e., A, X, Y, SAPO, ALPO, ...), were used as coating material on several substrates to obtain ‘smart’ layers (that respond selectively to the environment) able to offer a suitable functional action. Zeolite coating technology was applied effectively in several industrial purposes, e.g., catalysis processes [40,41], optic [42,43], adsorption [44,45], sensing [46,47] applications.

In the last two decades, several studies on anti-corrosive performances of zeolite based coatings were developed. This research approach is based on the opportunity to integrate in a synergistic way intrinsic characteristics of the zeolite as non-toxicity (advantageous for very stringent applications such as food or human health), thermal and chemical stability (crucial for severe environmental applications), and selectivity (in order to enhance the smart coating efficiency). This makes zeolite a promising and potentially effective structural filler for the development of high performance anti-corrosion composite coatings.

### 3. Zeolite-Based Anti-Corrosion Coatings

Over 15 years ago there was a triggered interest and improvement of knowledge in the production of zeolite-based films for its use as anti-corrosive protective coatings, thanks to the pioneering activities of Yan and its research group [48,49]. In these early works, the zeolite coating was obtained by direct synthesis on aluminum and steel alloys supports. Based on polarization electrochemical impedance

spectroscopy (EIS) analysis it was possible to evidence a reduction of corrosion current up to 4 orders of magnitude as compared to uncoated substrate and a high impedance magnitude at low frequency ( $10^9 \Omega \text{ cm}^2$ ). Furthermore, coupled to the good electrochemical performances, zeolite-based films showed a good adhesion, compactness, and mechanical and chemical stability, indicating them as effective alternative to conventional anti-corrosion coatings. The results also indicated that the zeolite coating approach could be directly extended to other metal or composite substrates [50].

The evidenced up-and-coming results, as environmentally friendly protective coatings, support the development of new research activities focused on optimizing and extending the applicability of this class of materials. In particular, Zheludkevich et al. [51] in 2012 proposed the use of zeolite as carrier of active inhibitor ions in functional self-healing coating. In parallel, Calabrese et al. [52,53], in the same period, evidenced an active barrier action of undoped zeolite coatings suggesting its applicability in severe critical environmental conditions. Subsequently, the improved knowledge in the corrosion protection mechanisms of zeolites further increased the interest on this subject. This has led more research groups, up to now, to start new research activities to better understand the protection mechanisms and to better define the capabilities and limits of the zeolite coatings.

Summarizing, depending on the support and purpose of use, different deposition techniques can be selected as suitable for obtaining anti-corrosion zeolite coating [54,55]. Synthesis techniques can be grouped in two main families: in situ crystallization coatings and composite zeolite coatings. In the former, a direct synthesis of zeolite on the metal substrate is obtained. In the latter, the zeolite is used as filler in a polymeric matrix with layer capabilities.

Among these techniques, sol-gel and in situ crystallization coatings are the most widely used. Sol-gel coatings are typically obtained starting from a colloidal solution (sol) that react forming an integrated crosslinked network (gel). In situ crystallization method allows the synthesis of a zeolite layer directly on the metal surface. This technology leads to a very effective coating/substrate interface, inducing a good adhesion with the metal support. Furthermore, by using this approach, it is possible to coat irregularly-shaped geometries, indicating it as a suitable and reliable coating technology for complex components. Details on the potential and effectiveness of pure zeolite coatings obtained by direct synthesis are reported in [25]. Although some troubles related to costs and technological scale-up issues have limited the development of this technology. Furthermore—notwithstanding the in-situ crystallization (e.g., by hydrothermal process) leading to well-adherent pure zeolite layers—low density, porous, or cracked coatings are often obtained during the synthesis process caused by a random and not-easily-controllable nucleation of zeolite crystals on the support [56,57].

#### 4. Composite Zeolite Coatings

The composite zeolite coatings are constituted mainly by two constituents: a filler and a matrix. Zeolite crystals obtained by using conventional synthesis process act as filler. The matrix is a bulk material in which the zeolite filler is embedded. Furthermore, the matrix provides an interface for binding and holding filler to obtain a continuous and homogeneous coating. It provides the transfer load improving adhesion with the substrate and cohesion among constituents and ensure the barrier properties of the coatings contributing to its durability and functionality in severe environmental conditions.

This approach, different from the direct synthesis one, is compatible to conventional paint and varnish technologies, and can use simple and easily scalable technologies without compromising the mechanical and electrochemical stability of the protective layer, making it an attractive solution for production companies.

The adoption of this technological solution allows the development of composite coatings where zeolite filler can exalt the protective barrier action acting as nano-containers for active corrosion inhibitor agents. The idea is to maintain the technological and functional advantage of paints and varnish preserving the high thermal stability of the zeolite observed in severe environmental conditions [51,58–60].

In such a context, in the last years, several research activities were being focused in improving the knowledge on anti-corrosion performances and protection mechanisms of composite zeolite coatings, proposing different deposition techniques and matrix types [61–64]. Particularly in the present review, the composite zeolite coatings technology were classified mainly in two categories: zeolite thermosetting polymer paints and sol-gel coatings, indicating these approaches as the most mature and suitable for their industrial field applicability.

#### 4.1. Zeolite Painting

Organic coatings are widely used for metal corrosion protection due to the high barrier capacity to ions, water, and oxygen diffusion through the protective layer. In recent years, a new challenge in the paint technology field was to provide coupled barrier protection with coatings able to selectively respond depending on external stimuli induced by operating environmental conditions. The target is to obtain smart painting formulation that triggers a release of an inhibitor only when the corrosion phenomenon occurs, inducing a self-healing action.

Padhy et al. [65] added NaY zeolites, exchanged with zinc metal ion, in an anticorrosive epoxy paint. The results highlighted that  $Zn^{2+}$  ion exchanged zeolite provides suitable anticorrosion performances, up to 16 days of immersion in 3.5 wt % NaCl solution. The impedance magnitude at low frequency was also three orders of magnitude higher than the unmodified coating. Similar results were observed in an epoxy coating functionalized with zeolite filler used as reservoir of active  $Ce^{3+}$  ions [66].

Although Devaki and Priya in [67] provided an inhibitory efficiency (IE, defined as percentage reduction of corrosion rate in zeolite-coated sample compared to uncoated one) of the zeolite-coated samples, after immersion in seawater for 2 months, of 93.74%, also by using undoped zeolite filler.

Ahmed et al. [59], investigating Zn, Ca, and Mg cation-exchanged zeolites as filler for an oil-modified soya-bean dehydrated castor oil alkyd resin paint, indicate that zeolites provide a reliable corrosion protection thanks to a coupled action: a physical corrosion protection thanks to a barrier action and a chemical protection due to the interaction of the zeolite surface with the acidic-modified alkyd resin used as matrix producing soaps which passivate the metal substrate.

More recently, Rassouli and coworkers assessed the active corrosion protection performances of epoxy ester coating filled with zeolite nanoparticles with zinc [68] or combined organic and inorganic inhibitors [69]. An active anti-corrosion capability was observed for the zeolite filled paint, probably due to a progressive release of inhibitors, providing also a suitable synergistic corrosion protection on coupled  $Zn^{2+}$ /mercaptobenzimidazole doped zeolite filled in the epoxy ester coating.

Similarly, a synergistic corrosion protection action was observed doping NaY zeolite with  $Ce^{3+}$  ions and 2-mercaptobenzothiazole added in a waterborne epoxy resin [70].

In parallel with the use of thermosetting polymeric binders, such as matrices for painting, an effective protective action on zeolite composite coating can also be obtained by using thermoplastic polymers able to interact to zeolite filler, such as polyaniline [71,72], which—being a conductive polymer—can use the electrodeposition technique in addition to the conventional ones with the opportunity to more effectively manage the thickness of the coating to be applied to the metal support [61,73].

The reliable active protection from corrosion offered by the doped zeolite with inhibiting agents can have a profitable effect in economic terms in the optimization of the painting formulation, potentially involving the complete substitution of the zinc phosphate with the doped zeolite, implying at the same time an improvement of the anticorrosive performances thanks to the inhibiting action offered by these pigments [58,62].

The self-healing properties of the zeolite composite paints is strictly related to the release capability of the inhibitor due to interaction with the electrolyte. It is worth noting that on this protection mechanism the environmental conditions, such as the pH of the electrolyte, play a relevant role on the inhibitory efficiency of the paint.

In such a context, Guo et al. [74] evidenced a rapid release of benzotriazole inhibitor onto scratched areas on metal surfaces under acidic conditions, providing a very high inhibition efficiency (99.4%). Instead, a limited release of inhibitor species (less than 4%) was observed in neutral environmental conditions.

Table 1 summarizes composite coating characteristics and main corrosion parameters of zeolite painting systems reported in the literature.  $I_{\text{cor}}$  is defined as the corrosion current calculated at open circuit potential (OCP). Furthermore the  $|Z|_{0.01 \text{ Hz}}$  indicates the impedance modulus of the surface at low frequency (0.01 Hz).

**Table 1.** Examples of literature review of anti-corrosion performances of zeolite painting systems.

Authors	Ref.	Year	Zeolite			Matrix	Substrate	Coating Thickness	Testing Electrolyte	$I_{cor}$ [A/cm <sup>2</sup> ]		Z  0.01 Hz [Ω/cm <sup>2</sup> ]		
			Type	Content	Inhibitor					Coating	Substrate	Coating	Substrate	
Olad et al.	[71]	2010	clinoptilolite	0%	none	polyaniline	iron	20 μm	3.5% NaCl	$7.5 \times 10^{-7}$	-	-	-	
				1%						$3.1 \times 10^{-5}$				
				3%						$1.0 \times 10^{-6}$				
				5%						$1.3 \times 10^{-6}$				
Olad et al.	[71]	2010	clinoptilolite	0%	none	polyaniline	iron	20 μm	1 M H <sub>2</sub> SO <sub>4</sub>	$5.6 \times 10^{-6}$	-	-	-	
				1%						$1.2 \times 10^{-5}$				
				3%						$1.4 \times 10^{-6}$				
				5%						$3.2 \times 10^{-6}$				
Olad et al.	[71]	2010	clinoptilolite	0%	none	polyaniline	iron	20 μm	1 M HCl	$7.5 \times 10^{-5}$	-	-	-	
				1%						$4.2 \times 10^{-5}$				
				3%						$3.1 \times 10^{-6}$				
				5%						$7.9 \times 10^{-6}$				
Padhy et al.	[65]	2015	Y	2%	none Zn	epoxy	mild steel	45 μm	3.5% NaCl	-	-	$8 \times 10^6$	-	
Zhang et al.	[66]	2016	MCM-22	-	none Ce	epoxy	Mg-Li alloy	50 μm	0.35% NaCl	-	-	$2 \times 10^7$	-	
Devaki et al.	[67]	2016	-	76%	none	-	mild steel	35 μm	3.5% NaCl	$3.0 \times 10^{-5}$	$8.3 \times 10^{-4}$	-	-	
Rassouli et al.	[68]	2017	X	0%	Zn	epoxy ester	mild steel	27 μm	3.5% NaCl	$1.1 \times 10^{-2}$	-	-	$1 \times 10^3$	-
				1%						$1.3 \times 10^{-3}$			$1 \times 10^{3.5}$	
Roselli et al.	[62]	2018	-	30%	Zn phosphate Ce	alkyd	SAE 1010 steel	70 μm	0.05 M NaCl	-	-	-	$1 \times 10^4$	-
Guo et al.	[74]	2018	ZIF-7	1%	none benzotriazole	epoxy	Q235 steel	70 μm	0.1 M HCl	-	-	-	$1 \times 10^6$	-
													$3.5 \times 10^4$	
Abdolah et al.	[70]	2018	Y	-	none Ce MBZ Ce + MBZ	epoxy	AA2024-T3	30 μm	0.05 M NaCl	-	-	-	$4.0 \times 10^4$	-
													$6 \times 10^5$	
													$1.0 \times 10^6$	
													$1.0 \times 10^6$	
Rassouli et al.	[69]	2018	X	1%	none MBI Zn MBI + Zn	epoxy ester	mild steel	28 μm	3.5% NaCl	-	-	-	$7.0 \times 10^6$	-
													$1 \times 10^{8.4}$	
													$1 \times 10^{8.1}$	
													$1 \times 10^9$	
Shabani et al.	[61]	2018	Y	1%	none	polyaniline	SS 304 SS 304	-	0.5 M HCl	$1 \times 10^{10.4}$	-	-	$5.8 \times 10^4$	$2.6 \times 10^2$
										$2.0 \times 10^{-5}$			$6.8 \times 10^{-5}$	$5.3 \times 10^{-6}$
Aziz et al.	[72]	2019	X	1%	none	polyaniline	SS316 Al Carbon steel	-	3.5% NaCl	$1.0 \times 10^{-6}$	-	-	$5.4 \times 10^{-6}$	-
										$1.0 \times 10^{-6}$			$8.4 \times 10^{-5}$	
										$3.2 \times 10^{-5}$			$7.7 \times 10^{-5}$	
										$2.4 \times 10^{-5}$			$7.7 \times 10^{-5}$	

MBZ: mercaptobenzothiazole. MBI: 2-mercaptobenzimidazole.

#### 4.2. Sol-Gel Coatings

The sol-gel coating technology is an alternative method that offers the possibility to deposit thin layers of binder-based zeolite coatings. By this approach, coating thickness usually in the range of 10–100  $\mu\text{m}$  by, e.g., controlling the viscosity of the liquid suspension and the dipping speed, can be obtained.

The technology is based on a dip coating deposition procedure (a scheme of the process is reported in Figure 2), where the metal part is dipped in a binder-zeolite solution followed usually by curing (depending on binder typology, in the range 60–150  $^{\circ}\text{C}$ ) in order to complete the cross-linking reactions in the matrix and to be sure that the optimal curing of the coating is reached.

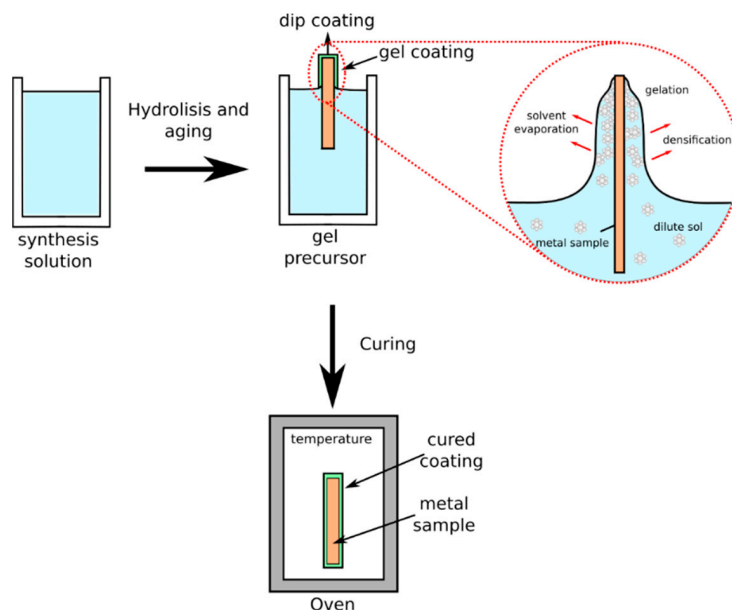


**Figure 2.** Scheme of a dip-coating process.

In the dip-coating process the uncoated sample is immersed in a liquid and then withdrawn with a well-defined withdrawal speed at controlled temperature and atmospheric conditions. During the process, the environmental conditions (atmosphere and temperature) control the solvent evaporation from the diluted sol. During this stage, a densification of the solution occurs, leading eventually to a gelation phenomenon, favored by the presence of solid filler, with the formation of a compact and homogeneous film well adherent to the substrate. The thickness of the coating is mainly defined by the picking speed, the filler content, and the viscosity of the liquid [75]. The adhesion with the substrate is guaranteed choosing a suitable binder matrix able to interact both to filler and substrate surface in order to offer high adhesion and cohesion of the constituted composite coating [76].

In such a context, the silane was widely used as suitable matrix to embed the zeolite grains, doped or undoped with corrosion inhibitors, in order to obtain an effective compact and defect free zeolite composite coating. Calabrese et al. [53] investigated the anti-corrosion performances of a SAPO-34 zeolite composite coating on an AA6061 aluminum alloy substrate. Filler content in the range 2000–8000 ppm of the silane matrix was evaluated. The results indicated that the corrosion current decreases up to three orders of magnitudes compared with the uncoated aluminum sample. Better results were observed by using 4000 ppm of SAPO-34 filler. Analogously, in the same period, Diaz et al. [60,77,78] assessed the addition of La-, Mo-, or Ce-enriched NaX zeolite nanocontainer to hybrid sol-gel silane based coating in order to enhance the corrosion resistance and performances. Their results evidenced that, after two aging weeks of immersion in 3.5% NaCl solution, the composite sol-gel film is stable and able to keep its protective action. These properties were related to rare earth ions, encapsulated in the NaX zeolite particles, released in the coating surface caused to an ion exchange with species involved in the corrosion process of the aluminum alloy substrate. Similar results

were obtained by Capri et al. [79] on a SAPO-34 zeolite filler doped with cerium ions. The chosen zeolite did not allow the ion exchange of ions as observed by Diaz [58,75,76], but allowed the active protection of the composite coating thanks to the sorption of cerium hydroxide on the reactive surface of SAPO-34 zeolite.

To effectively tailor the corrosion resistance efficiency of sol-gel zeolite coating Ferrer et al. [80] proposed a composite coating by using a hybrid tetraethoxysilane (TEOS)/epoxy matrix. In particular, NaY zeolites were doped combining cerium ions and diethyldithiocarbamate (DEDTC) inhibitors. The results provide, at first, a confirmation of the suitable release of corrosion inhibitors from the zeolite carrier system. Furthermore, it provides a new approach of functional sol-gel coatings, in which the self-healing mechanism acts with different release kinetics depending to the inhibitor species inoculated in the container. This expands the functionality of zeolite-based coating improving its selective release capabilities during aging time.

Despite previous articles, Calabrese et al. in [81] and [82] highlighted the opportunity to significantly enhance the barrier protection of the composite zeolite coating (on aluminum and magnesium substrate, respectively) by using a silane matrix filled with very high zeolite content (up to 90 wt %). These preliminary promising results were furthermore improved in terms of synthesis process and silane matrix modification [83,84] making it possible to reach a coating impedance five orders of magnitude higher than bare AA6061 aluminum alloy substrate ( $2 \times 10^9$  and  $2 \times 10^4 \Omega/\text{cm}^2$ , respectively).

More recently, Rassouli et al. [85] investigated different doping methods on NaX zeolite crystals to host  $\text{Zn}^{2+}$  and mercaptobenzimidazole inhibitors. A silane ( $\gamma$ -glycidoxypropyltri-methoxysilane, g-GPS, TEOS, and methyltriethoxysilane) was used as matrix for the sol-gel composite coating preparation. It was observed that the corrosion inhibition effect was influenced by the doping procedure, evidencing that the released inhibitors significantly reduces the corrosion phenomena on a carbon steel substrate cause to the formation of a protective layer induced by the inhibitor on its surface.

The choice of a silane matrix for the realization by sol-gel technique of zeolite composite coatings is strongly linked to the chemical affinity of the two constituents which involves obtaining a coating with an effective protection and durability in an aggressive environment.

The addition of zeolite filler in the silane matrix influences both cathodic and anodic reactions occurring on the metal alloy surface, inducing an effective protective action against corrosion phenomena.

Three main mechanisms act to enhance the corrosion resistance of silane-zeolite coatings:

- Inhibition action: The inhibition action can be related to a reaction of zeolite surface with the  $\text{OH}^-$  ions generated by the cathodic reaction that leads to the formation of  $\text{SiO}_3^-$  polar groups which are able to interact with the  $\text{Al}^{3+}$  ions, generated in the anodic area to form a passivating silica-alumina layer [86].
- Barrier action: The barrier protection offered by the silane-zeolite composite coatings is related to limited diffusion of aggressive species, through the coating, toward the metal substrate thanks to low liquid water permeability of silane matrix [87]. At the same time, the presence of zeolite filler in the silane layer increases the film thickness and reduces the layer porosity, exalting the anti-corrosion and barrier properties of the coating [88].
- Hydrophobic action: The surface hydrophobicity of the coating, that can be characterized by water contact angle above  $140^\circ$  [89], is due to the high chemical interaction between the composite constituents of the coating. In particular, the surface of the zeolite crystals is characterized by a large amount silanol functional groups that are able to create a chemical reaction with the silane matrix [90]. These Si-OH groups externally located in the zeolite particles act as preferential sites for the physical and chemical adsorption of the hydrolyzed silane molecules [91,92], reducing the surface polarity and the interaction with water molecules [93]. In fact, due to the functionalization of the zeolite with silane coupling agent, the hydrophobicity of the external surface can be easily triggered [94]. Furthermore, the high chemical affinity between zeolite filler and silane matrix could also increase the crosslinking density [95], thus limiting the hydrophilic sites in

the matrix and exalting the coating hydrophobicity [96]. Finally, caused by the reaction of the zeolite surface with the hydrolyzed silane groups, a strong covalent bond is formed between the two constituents and silane long alkyl chains tend to gather on the peripheral areas of the zeolite crystal. The resulting structure can therefore be characterized by functional micelles with a preferential orientation of hydrophobic alkyl chains, which reduce surface energy and enhance the hydrophobic properties of the coating [53].

In Table 2, a brief summary of literature articles focused on the sol-gel coatings filled with zeolite filler is reported. Details of composite formulation and corrosion protection performances of the coatings are shown.

**Table 2.** Examples of literature review of anti-corrosion performances of zeolite based sol-gel coatings.

Authors	Ref.	Year	Zeolite			Matrix	Substrate	Coating Thickness	Electrolyte	$I_{cor}$ (A/cm <sup>2</sup> )		Z  0.01 Hz (Ω/cm <sup>2</sup> )	
			Type	Content	Inhibitor					Coating	Substrate	Coating	Substrate
Calabrese et al.	[53]	2012	Y	2% 4% 8% 16%	none	TMS	AA6061	10 μm 10 μm 10 μm 10 μm	3.5% NaCl	$2 \times 10^{-5}$ $1 \times 10^{-5}$ $2 \times 10^{-6}$ $2 \times 10^{-5}$	$2 \times 10^{-5}$	–	–
Dias et al.	[60]	2012	X	–	none Ce	GLYMO + ZTP	AA2024-T3	1.5 μm	3.0% NaCl	–	–	$7 \times 10^5$ $7 \times 10^5$	$5 \times 10^5$
Dias et al.	[77]	2013	X	26.9% 26.9%	none Ce	GLYMO + ZTP	AA2024-T3	3.0 μm	0.05 M NaCl	–	–	$5 \times 10^6$ $5 \times 10^6$	$3 \times 10^6$
Ferrer et al.	[80]	2014	Y	10%	none Ce DEDTC Ce + DETC	GLYMO + TEOS + epoxy resin	AA2024-T3	100 μm	0.05 M NaCl	$4 \times 10^{-6}$ $4 \times 10^{-7}$ $2.5 \times 10^{-6}$ $1 \times 10^{-7}$ $2 \times 10^{-5}$ $3 \times 10^{-7}$ $7 \times 10^{-7}$ $5 \times 10^{-6}$	$5 \times 10^{-6}$	–	–
Calabrese et al.	[81]	2014	SAPO-34	60% 70% 80% 90%	none	TMS	AA6061	7 μm 8 μm 10 μm 15 μm	3.5% NaCl	$2 \times 10^{-10}$ $5 \times 10^{-11}$ $2 \times 10^{-11}$	$1.5 \times 10^{-5}$	$1.2 \times 10^5$ $1.9 \times 10^5$ $8 \times 10^5$ $3.7 \times 10^6$ $2 \times 10^5$ $4 \times 10^5$ $2 \times 10^5$ $3 \times 10^6$ $8 \times 10^5$ $5 \times 10^8$	$1.2 \times 10^4$
Dias et al.	[78]	2014	X	2%	none La Mo La + Mo	silane	AA2024-T3	3.0 μm	0.05 M NaCl	–	–	$2 \times 10^5$ $4 \times 10^5$ $2 \times 10^5$ $3 \times 10^6$	–
Capri et al.	[79]	2015	SAPO-34	80%	none Ce	TMS	AA6061	10 μm	3.5% NaCl	–	–	$8 \times 10^5$ $5 \times 10^8$	$2 \times 10^4$
Calabrese et al.	[83]	2016	SAPO-34	80%	none	TMS DMS + TMS OTS	AA6061	10 μm	3.5% NaCl	$2 \times 10^{-10}$ $5 \times 10^{-11}$ $2 \times 10^{-11}$	$2 \times 10^{-5}$	$1 \times 10^9$ $2 \times 10^9$ $2 \times 10^9$	$2 \times 10^4$
Calabrese et al.	[84]	2017	SAPO-34	80%	none	DMS + TMS	AA6061	15 μm	3.5% NaCl	$5 \times 10^{-11}$	$2 \times 10^{-5}$	$2 \times 10^9$	$1.2 \times 10^4$
Calabrese et al.	[82]	2018	SAPO-34	20% 40% 60% 80%	none	TMS	–	5 μm 7 μm 9 μm 11 μm	3.5% NaCl	–	–	$2 \times 10^5$ $1 \times 10^6$ $2 \times 10^7$ $2 \times 10^7$	$8 \times 10^3$
Rassolui et al.	[85]	2018	X	1	none Zn + MBI	MTES + TEOS + GLYMO	mild steel	–	3.5% NaCl	$1 \times 10^{-6}$ $5 \times 10^{-7}$	$1.4 \times 10^{-5}$	$1.5 \times 10^4$ $3 \times 10^4$	$0.7 \times 10^3$

TMS: N-propyl-trimethoxy-silane; GLYMO: 3-glycidyloxypropyl trimethoxysilane; ZTP: zirconium (IV) tetrapropoxide; DMS: dimethyl-dimethoxy-silane; OTS: octyltriethoxysilane; MTES: methyltriethoxysilane; TEOS: tetraethyl orthosilicate; DEDTC: sodium diethyldithiocarbamate trihydrate; MBI: 2-mercaptobenzimidazole.

It is worth noting that the anticorrosion performances of the composite zeolite coating extend on a wide range of values. This variability is related to differences in coating microstructure. A composite coating with low filler content is characterized by a thin layer microstructure, usually in the order of some  $\mu\text{m}$ . A possible morphology is shown in Figure 3a related to AA 2024 substrate coated with a hybrid sol-gel film filled with Ce doped 13X zeolite micro-particles (filler content 26.9 wt %) [77]. In the image, (1) identifies the sol-gel film, (2) an intermetallic particle, and (3) indicates zeolite microparticles in CeNaX sol-gel coating. For this coating formulation, the filler is not able to offer a relevant barrier protection to corrosion phenomena and its contribution is mainly limited to the inhibitor nano-container action.

Instead, the realization of zeolite coatings with a high filler content (Figure 3b shows an example for a coating with 70 wt % SAPO-34 zeolite filler on AA6061 support [81]), can obtain a coating with a suitable packing of the solid filler. As shown in cross-section image, the filler is well interconnected and 3-4 zeolite grains along the coating thickness can be identified. This implies, associated with the higher thickness (from 2  $\mu\text{m}$  to about 8  $\mu\text{m}$  for 26.9 wt % and 70 wt % filler content, respectively), an exaltation of the barrier properties of the coating so offering an effective protection from water and ionic species diffusion. This leads to an improvement in corrosion resistance and durability in an aggressive environment [83].

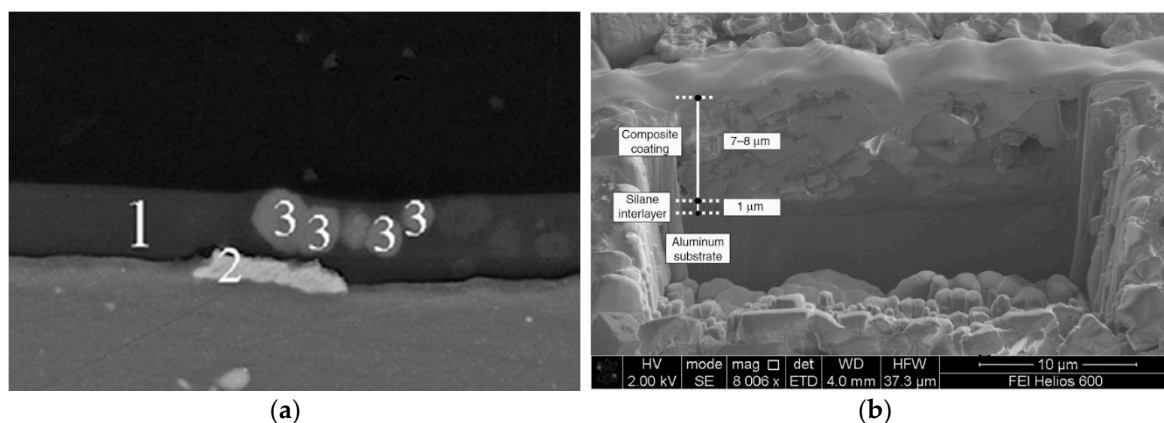


**Figure 3.** SEM image of composite zeolite coating with (a) 26.9 wt % of zeolite filler (Reprinted with permission from [77]. © 2013 Elsevier); and (b) 70 wt % of zeolite filler (Reprinted with permission from [81]. © 2014 Springer Nature).

Figure 4 better highlight these considerations, summarizing the increase of electrochemical impedance modulus at low frequency (0.1 HZ) with zeolite filler content, in accordance to review data reported in Table 2. Furthermore, the marker size is scaled to coating thickness. A progressive increase of impedance magnitude at increasing zeolite content can be observed. In particular for filler content lower than 20 wt %, the impedance modulus is in the range of  $10^4$ – $10^6 \Omega\cdot\text{cm}^2$ . Instead, for zeolite content above 70 wt %  $|Z|$  reach values up to  $10^9 \Omega\cdot\text{cm}^2$ , three order of magnitude higher than low filler content composite coating. At the same time, a progressive increase in thickness contributing to resistance and capacitance improvement in performances of the coating [81] can be demonstrated too.

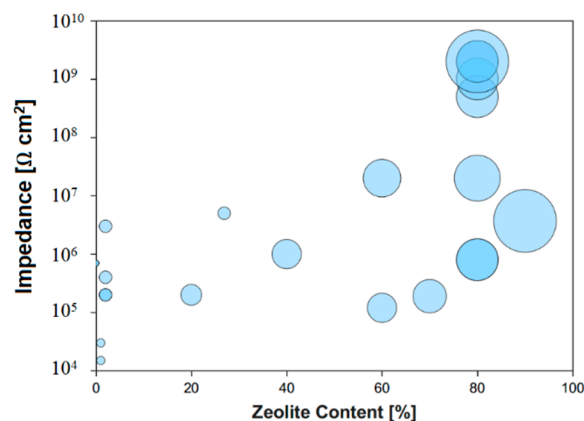


**Figure 4.** Variation of impedance modulus at 0.1 Hz and zeolite filler content (wt %). Marker size is scaled to coating thickness.

## 5. Anti-Corrosion Mechanisms of Zeolite Coatings

In order to better evaluate the anti-corrosion mechanisms of the zeolite coatings, a deeper evaluation on how this performance can be correlated to the coating structure and morphology is essential allowing to highlight in a targeted way the phenomena that trigger the barrier and/or self-repairing and self-healing mechanisms of the zeolite-based composite coatings.

### 5.1. Barrier Mechanisms

The barrier property that can reduce the substrate area available for anodic and cathodic reaction, is one of the main characteristics that influence the anti-corrosion performances of zeolite film. The barrier property increases if the inter- and intra-crystal porosity of the zeolite coating is reduced. To reduce the inter-crystalline porosity, and therefore to increase the resistance to mass diffusion along the thickness of the coating, a good packing of zeolite crystals during direct growth is required [52]. Furthermore, an active action of the zeolite layer can be hypothesized. In particular, according to Figure 5, in alkaline environments a significant decrease in corrosion rate can be observed. Calabrese et al. [56] related this interesting behavior observed at high pH to the protective action of a compact and dense aluminate layer deposited as corrosion product during the interaction of the zeolitic framework of the coating with the electrolyte solution. In particular, the sealing mechanism is related to a precipitation phenomenon triggered by the presence in the electrolyte solution of cations originating from dissociation of hydroxides present in alkaline electrolyte. These cations can react with corrosion products of the metal substrate producing insoluble salts. In saturated  $\text{Ca}(\text{OH})_2$  solution the formation of an insoluble surface layer of hydrated calcium aluminate  $\text{Ca}(\text{AlO}_2)_2 \cdot z\text{H}_2\text{O}$  was observed [97] as a consequence of the reaction of aluminate ions  $\text{AlO}_2^-$ , originating from zeolite dissolution, that are present at pH values above 12, with  $\text{Ca}^{2+}$  ions in the solution. This sealing mechanism stops any further corrosion reaction on the exposed metal substrate. Therefore, the good corrosion protection capabilities of zeolite coatings can be due to an active inhibitory action, according to the proposed scheme concerning the corrosion protection on defected area on zeolite-based coatings [84].

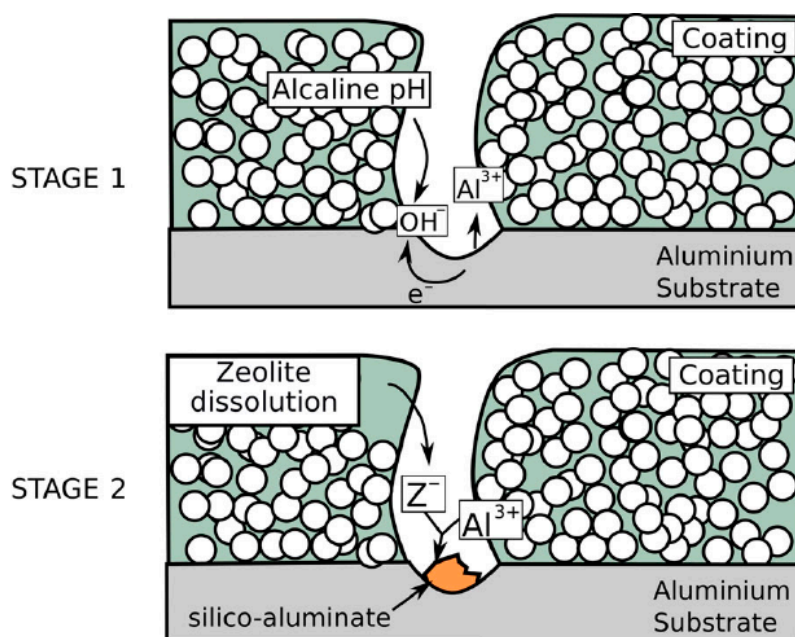


**Figure 5.** Scheme of corrosion protection on defected area on zeolite-based coatings [84]. Reprinted with permission from [84]. © 2017 Taylor & Francis.

In fact, when corrosion occurs on metal substrate in a defected area of a zeolite-based coating, locally the cathodic reaction favors the increase in the solution pH (stage 1 Figure 5). The  $\text{OH}^-$  groups could be adsorbed by functional species ( $>\text{Si}-\text{OH}$  and  $>\text{Al}-\text{OH}$ ) present on the zeolite framework both on internal channels and external surface. Such interaction leads to the formation of  $>\text{Si}-\text{O}$  and  $>\text{Al}-\text{O}$  groups with loose bonds to the mother lattice favoring, as a consequence, the detachment of zeolite framework portions [98]. The free  $>\text{Si}-\text{O}^{n-}$  and  $>\text{Al}-\text{O}^{n-}$  groups can then react with the metal cation generated due to dissolution phenomena at the anodic site (e.g.  $\text{Al}^{3+}$  ions), forming a passive silicate layer [99] that preserves the metal substrate from further corrosion processes (stage 2 in Figure 5) [84].

## 5.2. Active Mechanisms

The peculiar characteristic that distinguishes the zeolite-based coatings is the opportunity to couple to the barrier protection an active protection that selectively enhances the corrosion protection allowing to obtain the so-called smart coatings.

As previously illustrated, zeolite can be applied in composite coatings as ion-exchange micro- and meso-porous filler acting as nano-container of the corrosion inhibitor agent [100–102].

Zeolite carriers are able to be doped with inhibitor and healing agents. If the composite coating is locally damaged (e.g., due to cracks or scratches) the inhibitor entrapped in its framework structure is released promoting an active and self-healing process [103–105]. In the past, zeolite was applied as a nano-reservoir for functional antimicrobial agents, like silver ions, that are gradually released in the environment [106–108].

The advantage of a composite coating with multi-functional properties, such as antimicrobial and corrosion resistance, combined to the possibility to deposit it on several substrates, presents zeolite composite coatings as a reliable alternative to usual anti-corrosion coatings in specific industrial fields where unconventional or critical environmental conditions are required, such as in adsorption-based heat pumps or spacecraft applications [109–111].

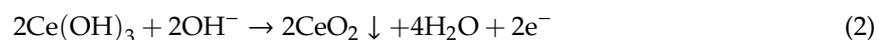
Several anti-corrosion approaches were applied in order to exalt the self-healing properties of zeolite doped coatings. In such a context, anti-corrosion paint has been developed by Deya et al. [100] who assessed a natural zeolite modified by molybdenyl ion exchange in order to improve the corrosion protection of steel alloy substrate. Based on their approach, when the electrolyte ions penetrate into

the coating, these ions are exchanged with molybdenyl cations, which generate molybdate anions following hydrolyzation. Molybdates are well known compounds with reliable inhibitor properties on steel alloy due to the formation of a compact and dense layer of ferrous molybdate [112,113].

Analogously, Dias et al. [60,77] showed very promising and suitable active anti-corrosion capability on sol-gel composite coatings filled with NaX zeolite nanoparticles ion exchanged with cerium cations. They highlighted that the driving protective mechanisms were activated by cerium hydroxide,  $\text{Ce}(\text{OH})_3$ , precipitation occurred on the cathodic areas of the substrate.

In particular, in order to evidence the cation-exchange effectiveness of zeolite particles Dias et al. [77] immersed in 0.5 M NaCl at different pH undoped and Ce-doped zeolite microparticles. They highlighted that, for the solution with the commercial zeolite (NaX), the pH values increased up to 8.5–8.9 just after 5 min of immersion and afterwards it stabilize on this value. Instead on the solution additive with Ce-enriched zeolite particles after 30 min of immersion, a stable pH value in the range 5.1–5.6 was observed, due to a concentration of  $\text{Ce}^{3+}$  (around 500 ppm) released on the solution.

Although, several anti-corrosion mechanisms were schemed in order to explain the inhibitory and self-healing capabilities of zeolite doped coatings. A large amount of them are related to the effect of pH modification induced in the anodic or cathodic areas. In fact, in correspondence of scratched or defected areas in the coating several micro-localized cells takes place. These micro electrochemical cells are characterized by anodic (where the metal dissolution occurs) and cathodic areas (where the oxygen reduction reaction takes place). In particular, for cerium-doped zeolite coatings, a relevant role is offered by the cathodic sites, where the pH can exceed 8. In alkaline environment, the formation of protective cerium oxide layer can be obtained, starting from cerium ions released from the zeolite doped nano-container, according to the reactions [114]



A self-healing mechanism of cerium-doped zeolite composite thermoresetting coatings is schemed in Figure 6. As proposed by Wang et al. [66], the cause of local surface damage in the coating was a result of the electrolyte solution reaches the coating, activating local corrosion of the substrate. In such a context, the presence of cathodic inclusion in the metal alloy substrate plays a relevant role in corrosion activation and inhibition mechanism stimulating the formation of galvanic corrosion cells at the metal/coating interface [60]. Anodic and cathodic areas are constituted. The process is activated thanks to the high amount of  $\text{Ce}^{3+}$  ions based on cation exchange properties of the zeolite in the composite coating [60,115]. The cerium ions are exchanged with cations present in the electrolyte solution (e.g.,  $\text{Na}^+$ ) favoring the release of the inhibitor locally in the defected area.

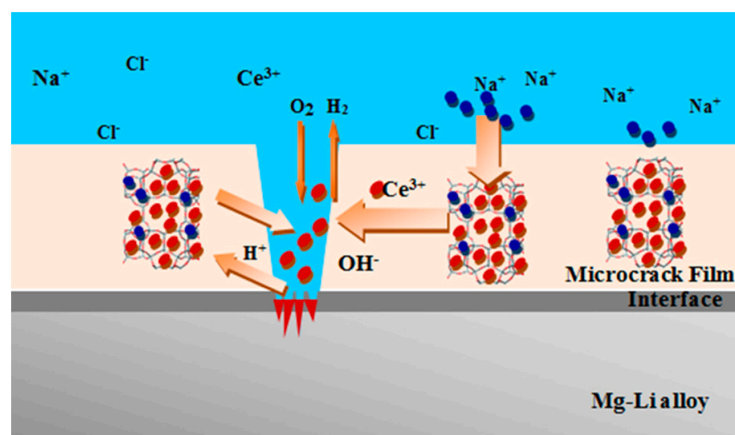


**Figure 6.** Scheme of the self-healing process on Ce-doped zeolite coatings [66]. Reprinted with permission from [66]. © 2016 Elsevier.

After the cerium ions release, according to Equation (1), they interact with the hydroxyl groups triggered by the cathodic oxygen reduction reaction [116] generating cerium hydroxide. The as-formed cerium hydroxide can act as protective layer providing slight self-repair action of the originated damaged area. Afterward, due to the alkaline environment on the cathodic area, the precipitation of cerium oxide,  $\text{CeO}_2$  is a consequence of a further interaction with the hydroxyl groups according to the reaction 2. The precipitation of a stable and compact  $\text{CeO}_2$  oxide significantly delays the activation and evolution corrosion phenomena, providing reliable coverage on the defective areas, thus improving the passivating action [117].

A similar self-healing mechanism was proposed by Guo et al. [74] in order to assess the anti-corrosion performances of zeolite coatings doped with benzotriazole (BTA) inhibitor compound. A scheme of the mechanism is reported in Figure 7.

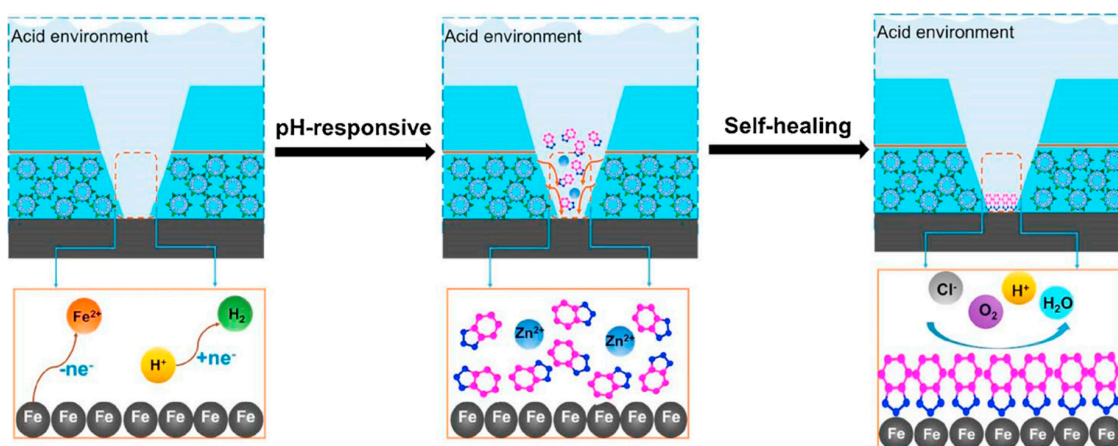


**Figure 7.** Schematic illustration for the self-healing mechanism of composite coating doped with benzotriazole activated zeolite nanoparticles [74]. Reprinted with permission from [74]. © 2019 Elsevier.

The self-healing mechanism of the polymer coatings is based on three steps. At first, in correspondence of a scratched zone, the electrolyte solution rapidly permeates along the scratch and interact with zeolite doped nanoparticles. Afterward, the BTA inhibitor is released from the zeolite container due to the pH-responsive nature of the metal–organic coordination. Finally, the inhibitor creates a compact layer in the cracked area, which prevents the substrate from further corrosion phenomena.

Consequently, the self-healing action of zeolite-based composite coatings can be acquired with different classes of inhibiting agents. In this context, a potentially effective approach is to dope the zeolite with different inhibitory molecules in order to provide a differential release of the encapsulated species in the zeolite framework, in order to enhance the progressive release and reliability of the active corrosion protection also in the medium and long term.

In such a context, Ferrer and coworkers [80] optimized a composite silane-epoxy zeolite coating. In particular, they doped NaY zeolite nanoparticles with coupled cerium and diethyldithiocarbamate (DEDTC) inhibitor agents in order to exalt the anti-corrosion performances and durability of the coating for protection of an AA2024-T3 substrate. Furthermore, a similar approach was applied by using molybdate and lanthanum ions [78]. In this case, the self-healing mechanism was explained by a gradual release of inhibitor ions from the doped zeolite inducing the formation of composite Mo-La-Na compounds with inhibitory properties on intermetallic precipitates in the aluminum matrix. All these results confirm the effectiveness of this approach for a suitable environmentally friendly and active corrosion protection.

A scheme that summarizes the double doping concept on zeolite-based coating is reported in Figure 8. Two different corrosion-inhibiting agents are encapsulated in the porous zeolite framework to offer a coupled protection effect. When, due to a local coating damage (favored by cathodic inclusions

in the alloy), the zeolite filler is exposed to the electrolyte medium (Figure 8, step 1), the inhibitor with faster kinetic release is leaked (inhibitor B in Figure 8, step 2). In this way, the metal substrate can be protected from corrosion phenomena in the short and medium term, thanks to the self-healing action of the first inhibitor. Afterward, the second inhibitor (inhibitor A in Figure 8, step 3) remaining hosted in the zeolite container favors its progressive release in the medium–long term, triggered by an ion exchange mechanism when the corrosion process advances. The second inhibitor need to have a higher inhibitor action in order to exalt at long time the corrosion protection when degradation phenomena could take place. The double-doping approach of zeolite containers is reliable only if the coupled inhibitor used in doping procedure is able to protect the substrate in synergistic way. In this case, an effective protection also at long aging time can be obtained thanks to a progressive and selective release during time of the different inhibitors. For example, in Ferrer et al. [78] the active corrosion protection of the composite sol-gel coating filled with double doped NaY zeolite is due at first to the release of the DEDTC in the short period. Because of the high affinity of the diethyldithiocarbamate to cathodic inclusions of the aluminum alloy (such as copper based intermetallic particles), a rapid surface corrosion protection can be obtained. Afterward, cerium released from the zeolite occurs more slowly through ion exchange mechanism between the cations from solution and cerium in the zeolite. The cerium has a higher inhibitory action and is able to offer a more effective protection up to long aging time [118]. Analogously, Rassouli et al. [69] assessed the effect of NaX zeolite particles loaded with coupled zinc cation and 2-mercaptobenzimidazole inhibitors evidencing an effective active corrosion protection, prolonging the coating lifetime.

This approach allows to significantly increase the potential applicability of the nano-porous zeolite particles as active inhibitor containers for corrosion protection of the metal substrates. Due to the coupled doping action of selective inhibitors, the zeolite composite coatings could provide a reliable multi-functional and long-term protective self-healing action.

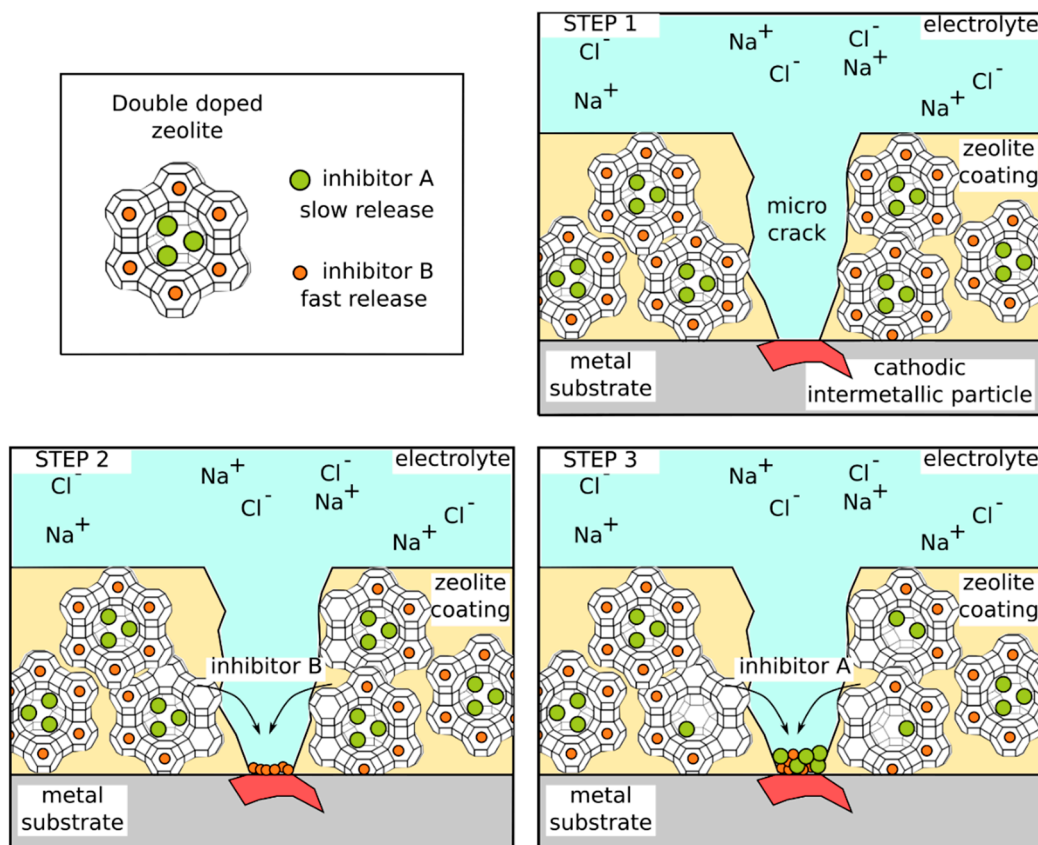


**Figure 8.** Scheme of the self-healing process of double doped zeolite on AA2024 metal substrate.

## 6. Conclusions and Future Trends

Anti-corrosion zeolite coatings is an emerging issue able to offer a reliable high performing and environmental friendly alternative to conventional chromate-based protective coatings. These types of coatings take advantage of the structural porosity of the zeolites, which can offer versatile functional properties such as molecular selectivity, ion and molecule storage capacity, high surface area and pore volume—which combined with excellent thermal and chemical stability—can extend its application fields in several industrial sectors. In such a context, in recent years, several research activities were focused on improving the knowledge of anti-corrosion performance and protection mechanisms of composite zeolite coatings, proposing different deposition techniques and matrix types. In particular, in the present review, the composite zeolite coating technology has been classified mainly in two categories: thermosetting and sol-gel coatings, indicating these approaches as the most mature and suitable for their industrial field applicability.

Three main mechanisms act to enhance the corrosion resistance of zeolite coatings:

- **Inhibition action:** The inhibition action is strictly related to the release capability of the inhibitor due to interaction with the electrolyte. It is worth noting that, on this protection mechanism, the environmental conditions, such as the pH of the electrolyte, play a relevant role in the inhibitory efficiency of the coating.
- **Barrier action:** The barrier protection is related to the limited diffusion of aggressive species, through the coating, toward the metal substrate thanks to low liquid water permeability of the matrix and, at the same time, to the reduction of the layer porosity due to the presence of zeolite filler that increases the film thickness, exalting the anti-corrosion properties of the coating.
- **Hydrophobic action:** The surface hydrophobicity of the coating, that can be characterized by water contact angle above  $140^\circ$ , is due to the high chemical interaction between the composite constituents of the coating. In particular, the surface of the zeolite crystals is characterized by a large amount silanol functional groups that are able to create a chemical reaction with the organic chains of the matrix, reducing the surface polarity and the interaction with water molecules.

An aspect that must always be taken into account is the economically sustainable productivity able to satisfy the potential growing demand from users of active protective coating systems. In this context, sol-gel technology has the requirements of flexibility, cost, and technological maturity that can satisfy these needs [119].

Critical issues are long term durability and functionality (e.g., self-healing and corrosion inhibitor actions). A limit of the composite sol-gel coating is the stability of corrosion protection performances and long aging time. Although effective protective properties are observed up to about one year of aging [79], further studies focused on the kinetic of inhibitors release and their interaction with coating and substrate during time are required [120]. The unwanted release of the inhibitors can reduce the durability of the self-healing properties. It is worth exploring functionality recovery in self-healing composites and studying improvement in mechanical properties of these smart composites over time [121].

Composite zeolite-based coatings still require further development in order to meet the various application challenges induced by the industrial sector. Furthermore, in addition to the aforementioned characteristics of long durability, other new relevant requirements need to be considered, such as aesthetics, environmental sustainability, and hydrophobicity [122–126].

Further progress on assessing defect free film growth in order to avoid defect issues on zeolite films should be value on the improvement of knowledge [127]. In such a context, the selection of a proper zeolite filler for each composite is required optimizing a specific zeolite structure as bench marking of the specific application [128].

Multi-functional coating is a really attractive technology able to combine on-demand corrosion protection to specific functionalities such as biocompatibility, electrical conductivity, self-diagnosis extending the research field interest promisingly in biomedical and coating sensors applications [129–131]. This approach of future surface engineering will be extended by the improved knowledge and experience on nano-materials, benefiting the capability and accelerating the applicability of sol-gel composite zeolite coatings.

**Author Contributions:** Conceptualization, L.C. and E.P.; Validation, L.C. and E.P.; Formal analysis, L.C.; Investigation, L.C.; Data curation, L.C.; Writing—original draft preparation, L.C.; Writing—review and editing, E.P.; Visualization, L.C.; Supervision, E.P.

**Funding:** This research received no external funding.

**Conflicts of Interest:** The authors declare no conflict of interest.

## References

1. Davis, J.R. *Surface Engineering for Corrosion and Wear Resistance*; ASM International: Cleveland, OH, USA, 2001; ISBN 1615030727.
2. Li, Y.; Li, L.; Yu, J. Applications of zeolites in sustainable chemistry. *Chem* **2017**, *3*, 928–949. [[CrossRef](#)]
3. Montemor, M.F. Functional and smart coatings for corrosion protection: A review of recent advances. *Surf. Coat. Technol.* **2014**, *258*, 17–37. [[CrossRef](#)]
4. Zheng, H.; Shao, Y.; Wang, Y.; Meng, G.; Liu, B. Reinforcing the corrosion protection property of epoxy coating by using graphene oxide-poly (urea-formaldehyde) composites. *Corros. Sci.* **2017**, *123*, 267–277. [[CrossRef](#)]
5. Tavandashti, N.P.; Ghorbani, M.; Shojaei, A.; Mol, J.M.C.; Terry, H.; Baert, K.; Gonzalez-Garcia, Y. Inhibitor-loaded conducting polymer capsules for active corrosion protection of coating defects. *Corros. Sci.* **2016**, *112*, 138–149. [[CrossRef](#)]
6. Sastri, V.S. *Green Corrosion Inhibitors: Theory and Practice*; Wiley: Singapore, 2011; ISBN 9780470452103.
7. Forsyth, M.; Hinton, B. *Rare Earth-Based Corrosion Inhibitors*; Woodhead Publishing: Cambridge, OK, USA, 2014; ISBN 9780857093585.
8. Yasakau, K.A.; Zheludkevich, M.L.; Lamaka, S.V.; Ferreira, M.G. Mechanism of corrosion inhibition of AA2024 by rare-earth compounds. *J. Phys. Chem. B* **2006**, *110*, 5515–5528. [[CrossRef](#)] [[PubMed](#)]
9. Garcia-Heras, M.; Jimenez-Morales, A.; Casal, B.; Galvan, J.C.; Radzki, S.; Villegas, M.A. Preparation and electrochemical study of cerium-silica sol-gel thin films. *J. Alloys Compd.* **2004**, *380*, 219–224. [[CrossRef](#)]
10. Khramov, A.N.; Voevodin, N.N.; Balbyshev, V.N.; Mantz, R.A. Sol-gel-derived corrosion-protective coatings with controllable release of incorporated organic corrosion inhibitors. *Thin Solid Films* **2005**, *483*, 191–196. [[CrossRef](#)]
11. Shchukin, D.G.; Zheludkevich, M.; Yasakau, K.; Lamaka, S.; Ferreira, M.G.S.; Möhwald, H. Layer-by-layer assembled nanocontainers for self-healing corrosion protection. *Adv. Mater.* **2006**, *18*, 1672–1678. [[CrossRef](#)]
12. Grigoriev, D.; Shchukina, E.; Shchukin, D.G. Nanocontainers for self-healing coatings. *Adv. Mater. Interfaces* **2017**, *4*, 1600318. [[CrossRef](#)]
13. Borisova, D.; Möhwald, H.; Shchukin, D.G. Mesoporous silica nanoparticles for active corrosion protection. *ACS Nano* **2011**, *5*, 1939–1946. [[CrossRef](#)]
14. Nesterova, T.; Dam-Johansen, K.; Pedersen, L.T.; Kiil, S. Microcapsule-based self-healing anticorrosive coatings: Capsule size, coating formulation, and exposure testing. *Prog. Org. Coat.* **2012**, *75*, 309–318. [[CrossRef](#)]
15. García, S.J.; Fischer, H.R.; van der Zwaag, S. A critical appraisal of the potential of self healing polymeric coatings. *Prog. Org. Coat.* **2011**, *72*, 211–221. [[CrossRef](#)]
16. Williams, G.; McMurray, H.N.; Loveridge, M.J. Inhibition of corrosion-driven organic coating disbondment on galvanised steel by smart release group II and Zn (II)—Exchanged bentonite pigments. *Electrochim. Acta* **2010**, *55*, 1740–1748. [[CrossRef](#)]
17. Ghazi, A.; Ghasemi, E.; Mahdavian, M.; Ramezanzadeh, B.; Rostami, M. The application of benzimidazole and zinc cations intercalated sodium montmorillonite as smart ion exchange inhibiting pigments in the epoxy ester coating. *Corros. Sci.* **2015**, *94*, 207–217. [[CrossRef](#)]

18. Snihirova, D.; Lamaka, S.V.; Taryba, M.; Salak, A.N.; Kallip, S.; Zheludkevich, M.L.; Ferreira, M.G.S.; Montemor, M.F. Hydroxyapatite microparticles as feedback-active reservoirs of corrosion inhibitors. *ACS Appl. Mater. Interfaces* **2010**, *2*, 3011–3022. [[CrossRef](#)]
19. Dong, C.; Zhang, M.; Xiang, T.; Yang, L.; Chan, W.; Li, C. Novel self-healing anticorrosion coating based on L-valine and MBT-loaded halloysite nanotubes. *J. Mater. Sci.* **2018**, *53*, 7793–7808. [[CrossRef](#)]
20. Wang, M.; Liu, M.; Fu, J. An intelligent anticorrosion coating based on pH-responsive smart nanocontainers fabricated via a facile method for protection of carbon steel. *J. Mater. Chem. A* **2015**, *3*, 6423–6431. [[CrossRef](#)]
21. Maia, F.; Tedim, J.; Lisenkov, A.D.; Salak, A.N.; Zheludkevich, M.L.; Ferreira, M.G. Silica nanocontainers for active corrosion protection. *Nanoscale* **2012**, *4*, 1287–1298. [[CrossRef](#)]
22. Hollamby, M.J.; Fix, D.; Dönch, I.; Borisova, D.; Möhwald, H.; Shchukin, D. Hybrid polyester coating incorporating functionalized mesoporous carriers for the holistic protection of steel surfaces. *Adv. Mater.* **2011**, *23*, 1361–1365. [[CrossRef](#)]
23. Borisova, D.; Akçakayran, D.; Schenderlein, M.; Möhwald, H.; Shchukin, D.G. Nanocontainer-based anticorrosive coatings: Effect of the container size on the self-healing performance. *Adv. Funct. Mater.* **2013**, *23*, 3799–3812. [[CrossRef](#)]
24. Wei, H.; Wang, Y.; Guo, J.; Shen, N.Z.; Jiang, D.; Zhang, X.; Yan, X.; Zhu, J.; Wang, Q.; Shao, L.; et al. Advanced micro/nanocapsules for self-healing smart anticorrosion coatings. *J. Mater. Chem. A* **2015**, *3*, 469–480. [[CrossRef](#)]
25. Calabrese, L. Anticorrosion behavior of zeolite coatings obtained by in situ crystallization: A critical review. *Materials* **2018**, *12*, 59. [[CrossRef](#)] [[PubMed](#)]
26. Javierre, E. Modeling self-healing mechanisms in coatings: Approaches and perspectives. *Coatings* **2019**, *9*, 122. [[CrossRef](#)]
27. Zhang, F.; Ju, P.; Pan, M.; Zhang, D.; Huang, Y.; Li, G.; Li, X. Self-healing mechanisms in smart protective coatings: A review. *Corros. Sci.* **2018**, *144*, 74–88. [[CrossRef](#)]
28. Zagorodni, A.A. *Ion Exchange Materials: Properties and Applications*; Elsevier: Oxford, UK, 2006; ISBN 9780080467535.
29. Mahesh, M.; Thomas, J.; Arun Kumar, K.; Bhopale, B.S.; Suresh, N.V.; Vaid, S.K.; Sahu, S.K. Zeolite farming: A sustainable agricultural prospective. *Int. J. Curr. Microbiol. Appl. Sci.* **2018**, *7*, 2912–2924. [[CrossRef](#)]
30. Ayele, L.; Pérez-Pariente, J.; Chebude, Y.; Diaz, I. Synthesis of zeolite A using kaolin from Ethiopia and its application in detergents. *New J. Chem.* **2016**, *40*, 3440–3446. [[CrossRef](#)]
31. Ghasemi, Z.; Sourinejad, I.; Kazemian, H.; Rohani, S. Application of zeolites in aquaculture industry: A review. *Rev. Aquac.* **2018**, *10*, 75–95. [[CrossRef](#)]
32. Kosinov, N.; Gascon, J.; Kapteijn, F.; Hensen, E.J.M. Recent developments in zeolite membranes for gas separation. *J. Memb. Sci.* **2016**, *499*, 65–79. [[CrossRef](#)]
33. Mandal, S.; Planells, A.D.; Hunt, H.K. Impact of deposition and laser densification of Silicalite-1 films on their optical characteristics. *Microporous Mesoporous Mater.* **2016**, *223*, 68–78. [[CrossRef](#)]
34. Lew, C.M.; Cai, R.; Yan, Y. Zeolite thin films: From computer chips to space stations. *Acc. Chem. Res.* **2010**, *43*, 210–219. [[CrossRef](#)]
35. Katariya, M.N.; Jana, A.K.; Parikh, P.A. Corrosion inhibition effectiveness of zeolite ZSM-5 coating on mild steel against various organic acids and its antimicrobial activity. *J. Ind. Eng. Chem.* **2013**, *19*, 286–291. [[CrossRef](#)]
36. Hamciuc, C.; Hamciuc, E.; Popovici, D.; Danaila, A.I.; Butnaru, M.; Rambu, C.; Carp-Carare, C.; Kalvachev, Y. Biocompatible poly (ether-ether-ketone)/Ag-zeolite L composite films with antimicrobial properties. *Mater. Lett.* **2018**, *212*, 339–342. [[CrossRef](#)]
37. Fernández, A.; Soriano, E.; Hernández-Muñoz, P.; Gavara, R. Migration of antimicrobial silver from composites of polylactide with silver zeolites. *J. Food Sci.* **2010**, *75*, E186–E193. [[CrossRef](#)] [[PubMed](#)]
38. Calabrese, L.; Bonaccorsi, L.; Freni, A.; Proverbio, E. Synthesis of SAPO-34 zeolite filled macrocellular foams for adsorption heat pump applications: A preliminary study. *Appl. Therm. Eng.* **2017**, *124*, 1312–1318. [[CrossRef](#)]
39. Bonaccorsi, L.; Bruzzaniti, P.; Calabrese, L.; Freni, A.; Proverbio, E.; Restuccia, G. Synthesis of SAPO-34 on graphite foams for adsorber heat exchangers. *Appl. Therm. Eng.* **2013**, *61*, 848–852. [[CrossRef](#)]

40. Caro, J.; Noack, M.; Kölsch, P.; Schäfer, R. Zeolite membranes-state of their development and perspective. *Microporous Mesoporous Mater.* **2000**, *38*, 3–24. [[CrossRef](#)]
41. Jeon, M.Y.; Kim, D.; Kumar, P.; Lee, P.S.; Rangnekar, N.; Bai, P.; Shete, M.; Elyassi, B.; Lee, H.S.; Narasimharao, K.; et al. Ultra-selective high-flux membranes from directly synthesized zeolite nanosheets. *Nature* **2017**, *543*, 690–694. [[CrossRef](#)] [[PubMed](#)]
42. Cao, L.; Hao, H.; Dutta, P.K. Fabrication of high-performance antifogging and antireflective coatings using faujasitic nanozeolites. *Microporous Mesoporous Mater.* **2018**, *263*, 62–70. [[CrossRef](#)]
43. Zhang, J.; Yu, J. Layer-by-layer approach to superhydrophobic zeolite antireflective coatings. *CJC* **2018**, *36*, 51–54. [[CrossRef](#)]
44. Bonaccorsi, L.; Calabrese, L.; Freni, A.; Proverbio, E. Hydrothermal and microwave synthesis of SAPO (CHA) zeolites on aluminium foams for heat pumping applications. *Microporous Mesoporous Mater.* **2013**, *167*, 30–37. [[CrossRef](#)]
45. Tatlier, M. Performances of MOF vs. zeolite coatings in adsorption cooling applications. *Appl. Therm. Eng.* **2017**, *113*, 290–297. [[CrossRef](#)]
46. Snelders, D.J.M.; Valega Mackenzie, F.O.; Boersma, A.; Peeters, R.H.M. Zeolites as coating materials for Fiber Bragg Grating chemical sensors for extreme conditions. *Sens. Actuators B Chem.* **2016**, *235*, 698–706. [[CrossRef](#)]
47. Huang, Q.; Wang, J.; Sun, Y.; Li, X.; Wang, X.; Zhao, Z. Gas-sensing properties of composites of Y-zeolite and SnO<sub>2</sub>. *J. Mater. Sci.* **2018**, *53*, 6729–6740. [[CrossRef](#)]
48. Cheng, X.; Wang, Z.; Yan, Y. Corrosion-resistant zeolite coatings by in situ crystallization. *Electrochim. Solid-State Lett.* **2001**, *4*, B23–B26. [[CrossRef](#)]
49. Mitra, A.; Wang, Z.; Cao, T.; Wang, H.; Huang, L.; Yan, Y. Synthesis and corrosion resistance of high-silica zeolite MTW, BEA, and MFI coatings on steel and aluminum. *J. Electrochem. Soc.* **2002**, *149*, B472–B478. [[CrossRef](#)]
50. Cai, R.; Yan, Y. Corrosion-resistant zeolite coatings. *Corrosion* **2008**, *64*, 271–278. [[CrossRef](#)]
51. Zheludkevich, M.L.; Tedim, J.; Ferreira, M.G.S. “Smart” coatings for active corrosion protection based on multi-functional micro and nanocontainers. *Electrochim. Acta* **2012**, *82*, 314–323. [[CrossRef](#)]
52. Bonaccorsi, L.; Calabrese, L.; Proverbio, E. Low temperature single-step synthesis of zeolite Y coatings on aluminium substrates. *Microporous Mesoporous Mater.* **2011**, *144*, 40–45. [[CrossRef](#)]
53. Calabrese, L.; Bonaccorsi, L.; Proverbio, E. Corrosion protection of aluminum 6061 in NaCl solution by silane-zeolite composite coatings. *J. Coat. Technol. Res.* **2012**, *9*, 597–607. [[CrossRef](#)]
54. Bein, T. Synthesis and applications of molecular sieve layers and membranes. *Chem. Mater.* **1996**, *8*, 1636–1653. [[CrossRef](#)]
55. Zaarour, M.; Dong, B.; Naydenova, I.; Retoux, R.; Mintova, S. Progress in zeolite synthesis promotes advanced applications. *Microporous Mesoporous Mater.* **2014**, *189*, 11–21. [[CrossRef](#)]
56. Calabrese, L.; Bonaccorsi, L.; Pietro, D.D.; Proverbio, E. Effect of process parameters on behaviour of zeolite coatings obtained by hydrothermal direct synthesis on aluminium support. *Ceram. Int.* **2014**, *40*, 12837–12845. [[CrossRef](#)]
57. Dong, Y.; Peng, Y.; Wang, G.; Wang, Z.; Yan, Y. Corrosion-resistant zeolite silicalite-1 coatings synthesized by seeded growth. *Ind. Eng. Chem. Res.* **2012**, *51*, 3646–3652. [[CrossRef](#)]
58. Romagnoli, R.; del Amo, B.; Revuelta, M.; Roselli, S.; Deyá, C.; Bellotti, N. Lanthanum-exchanged zeolite and clay as anticorrosive pigments for galvanized steel. *J. Rare Earths* **2014**, *32*, 352–359.
59. Ahmed, N.M.; Emira, H.S.; Selim, M.M. Anticorrosive performance of ion-exchange zeolites in alkyd-based paints. *Pigment Resin Technol.* **2011**, *40*, 91–99. [[CrossRef](#)]
60. Dias, S.A.S.; Lamaka, S.V.; Nogueira, C.A.; Diamantino, T.C.; Ferreira, M.G.S. Sol-gel coatings modified with zeolite fillers for active corrosion protection of AA2024. *Corros. Sci.* **2012**, *62*, 153–162. [[CrossRef](#)]
61. Shabani-nooshabadi, M.; Allahyary, E.; Jafari, Y. Enhanced anti-corrosive properties of electrosynthesized polyaniline/zeolite nanocomposite coatings on steel. *J. Nanostructure* **2018**, *8*, 131–143.
62. Roselli, S.; Deyá, C.; Revuelta, M.; Di Sarli, A.R.; Romagnoli, R. Zeolites as reservoirs for Ce (III) as passivating ions in anticorrosion paints. *Corros. Rev.* **2018**, *36*, 305–322. [[CrossRef](#)]
63. Rassouli, L.; Naderi, R.; Mahdavian, M.; Arabi, A.M. Synthesis and characterization of zeolites for anti-corrosion application: The effect of precursor and hydrothermal treatment. *J. Mater. Eng. Perform.* **2018**, *27*, 4625–4634. [[CrossRef](#)]

64. Al-Subaie, M.S.M.; Al-Turkustani, A.M.A.; Selvin, R.; Al-Mhayawi, S.R. Anticorrosion nanocrystalline beta zeolite thin film for advanced applications. *J. Chem.* **2015**, *2015*, 693730. [[CrossRef](#)]
65. Padhy, R.R.; Shaw, R.; Tiwari, S.; Tiwari, S.K. Ultrafine nanocrystalline mesoporous NaY zeolites from fly ash and their suitability for eco-friendly corrosion protection. *J. Porous Mater.* **2015**, *22*, 1483–1494. [[CrossRef](#)]
66. Wang, J.; Zhang, T.; Zheng, X.; Zhu, Y.; Yan, Y.; Zhang, M.; Shchukin, D.G.; Li, C.; Wang, Y.; Song, D. Smart epoxy coating containing Ce-MCM-22 zeolites for corrosion protection of Mg-Li alloy. *Appl. Surf. Sci.* **2016**, *369*, 384–389. [[CrossRef](#)]
67. Devaki, H.; Priya, P.G. Corrosion studies using zeolite synthesized from fly ash. *Indian J. Sci. Technol.* **2016**, *9*, 93147. [[CrossRef](#)]
68. Rassouli, L.; Naderi, R.; Mahdavian, M. The role of micro/nano zeolites doped with zinc cations in the active protection of epoxy ester coating. *Appl. Surf. Sci.* **2017**, *423*, 571–583. [[CrossRef](#)]
69. Rassouli, L.; Naderi, R.; Mahdavian, M. Study of the active corrosion protection properties of epoxy ester coating with zeolite nanoparticles doped with organic and inorganic inhibitors. *J. Taiwan Inst. Chem. Eng.* **2018**, *85*, 207–220. [[CrossRef](#)]
70. Abdollah Zadeh, M.; Tedim, J.; Zheludkevich, M.; van der Zwaag, S.; Garcia, S.J. Synergetic active corrosion protection of AA2024-T3 by 2D-anionic and 3D-cationic nanocontainers loaded with Ce and mercaptobenzothiazole. *Corros. Sci.* **2018**, *135*, 35–45. [[CrossRef](#)]
71. Olad, A.; Naseri, B. Preparation, characterization and anticorrosive properties of a novel polyaniline/clinoptilolite nanocomposite. *Prog. Org. Coat.* **2010**, *67*, 233–238. [[CrossRef](#)]
72. Abdel Aziz, A.H.; Jamil, T.S.; Shalaby, M.S.; Shaban, A.M.; Souaya, E.R.; Abdel Ghany, N.A. Application of (polyaniline/zeolite X) composite as anticorrosion coating for energy recovery devices in RO desalination water plants. *Int. J. Ind. Chem.* **2019**, *10*, 175–191. [[CrossRef](#)]
73. Shabani-Nooshabadi, M.; Mollahoseiny, M.; Jafari, Y. Electropolymerized coatings of polyaniline on copper by using the galvanostatic method and their corrosion protection performance in HCl medium. *Surf. Interface Anal.* **2014**, *46*, 472–479. [[CrossRef](#)]
74. Guo, Y.; Wang, J.; Zhang, D.; Qi, T.; Li, G.L. pH-responsive self-healing anticorrosion coatings based on benzotriazole-containing zeolitic imidazole framework. *Colloids Surf. A Physicochem. Eng. Asp.* **2018**, *561*, 1–8. [[CrossRef](#)]
75. Brinker, C.J.; Frye, G.C.; Hurd, A.J.; Ashley, C.S. Fundamentals of sol-gel dip coating. *Thin Solid Films* **1991**, *201*, 97–108. [[CrossRef](#)]
76. Thibault, M.; Bavay, J.; Hernandez, J.; Leroy, J.-M. Adhesion improvement mechanism of sol-gel silicone coatings. *Surf. Eng.* **1998**, *14*, 256–258. [[CrossRef](#)]
77. Dias, S.A.S.; Marques, A.; Lamaka, S.V.; Simões, A.; Diamantino, T.C.; Ferreira, M.G.S. The role of Ce (III)-enriched zeolites on the corrosion protection of AA2024-T3. *Electrochim. Acta* **2013**, *112*, 549–556. [[CrossRef](#)]
78. Dias, S.A.S.; Lamaka, S.V.; Diamantino, T.C.; Ferreira, M.G.S. Synergistic protection against corrosion of AA2024-T3 by sol-gel coating modified with La and Mo-enriched zeolites. *J. Electrochem. Soc.* **2014**, *161*, C215–C222. [[CrossRef](#)]
79. Capri, A.; Calabrese, L.; Bonaccorsi, L.; Proverbio, E. Corrosion resistance of cerium based silane-zeolite coatings on AA6061. *Solid State Phenom.* **2015**, *227*, 163–166. [[CrossRef](#)]
80. Ferrer, E.L.; Rollon, A.P.; Mendoza, H.D.; Lafont, U.; Garcia, S.J. Double-doped zeolites for corrosion protection of aluminium alloys. *Microporous Mesoporous Mater.* **2014**, *188*, 8–15. [[CrossRef](#)]
81. Calabrese, L.; Bonaccorsi, L.; Capri, A.; Proverbio, E. Electrochemical behavior of hydrophobic silane-zeolite coatings for corrosion protection of aluminum substrate. *J. Coat. Technol. Res.* **2014**, *11*, 883–898. [[CrossRef](#)]
82. Calabrese, L.; Capri, A.; Proverbio, E. Anti-corrosion performances of hybrid silane coatings on AZ31 alloy. *Anti-Corrosion Methods Mater.* **2018**, *65*, 317–324. [[CrossRef](#)]
83. Calabrese, L.; Bonaccorsi, L.; Capri, A.; Proverbio, E. Assessment of hydrophobic and anticorrosion properties of composite silane-zeolite coatings on aluminum substrate. *J. Coat. Technol. Res.* **2016**, *13*, 287–297. [[CrossRef](#)]
84. Calabrese, L.; Bonaccorsi, L.; Capri, A.; Proverbio, E. Enhancement of the hydrophobic and anti-corrosion properties of a composite zeolite coating on Al6061 substrate by modification of silane matrix. *Corros. Eng. Sci. Technol.* **2017**, *52*, 61–72. [[CrossRef](#)]

85. Rassouli, L.; Naderi, R.; Mahdavian, M. Study of the impact of sequence of corrosion inhibitor doping in zeolite on the self-healing properties of silane sol-gel film. *J. Ind. Eng. Chem.* **2018**, *66*, 221–230. [[CrossRef](#)]
86. Palanivel, V.; Zhu, D.; van Ooij, W.J. Nanoparticle-filled silane films as chromate replacements for aluminum alloys. *Prog. Org. Coat.* **2003**, *47*, 384–392. [[CrossRef](#)]
87. Woo, R.S.C.; Zhu, H.; Chow, M.M.K.; Leung, C.K.Y.; Kim, J.K. Barrier performance of silane-clay nanocomposite coatings on concrete structure. *Compos. Sci. Technol.* **2008**, *68*, 2828–2836. [[CrossRef](#)]
88. Montemor, M.F.; Cabral, A.M.; Zheludkevich, M.L.; Ferreira, M.G.S. The corrosion resistance of hot dip galvanized steel pretreated with Bis-functional silanes modified with microsilica. *Surf. Coat. Technol.* **2006**, *200*, 2875–2885. [[CrossRef](#)]
89. Calabrese, L.; Bonaccorsi, L.; Capri, A.; Proverbio, E. Adhesion aspects of hydrophobic silane zeolite coatings for corrosion protection of aluminium substrate. *Prog. Org. Coat.* **2014**, *77*, 1341–1350. [[CrossRef](#)]
90. Bonaccorsi, L.; Bruzzaniti, P.; Calabrese, L.; Proverbio, E. Organosilanes functionalization of alumino-silica zeolites for water adsorption applications. *Microporous Mesoporous Mater.* **2016**, *234*, 113–119. [[CrossRef](#)]
91. Hou, J.; Jiang, Q. Preparation of nanosized NaA zeolite and its surface modification by KH-550. *Mater. Sci.* **2019**, *36*, 638–643. [[CrossRef](#)]
92. Matsumoto, A.; Tsutsumi, K.; Schumacher, K.; Unger, K.K. Surface functionalization and stabilization of mesoporous silica spheres by silanization and their adsorption characteristics. *Langmuir* **2002**, *18*, 4014–4019. [[CrossRef](#)]
93. Bonaccorsi, L.; Calabrese, L.; Alioto, S.; Bruzzaniti, P.; Proverbio, E. Surface silanation of alumina-silica zeolites for adsorption heat pumping. *Renew. Energy* **2017**, *110*, 79–86. [[CrossRef](#)]
94. Wang, X.G.; Fang, X.; Che, S.; Du, T.; Liu, L.Y. Preparation of hydrophobic zeolite 13X@SiO<sub>2</sub> and their adsorption properties of CO<sub>2</sub> and H<sub>2</sub>O. *Adv. Mater. Res.* **2014**, *1053*, 311–316. [[CrossRef](#)]
95. Lee, J.; Lee, S.; Kim, S. Surface tension of silane treated natural zeolite. *Mater. Chem. Phys.* **2000**, *63*, 251–255. [[CrossRef](#)]
96. Deymier, P.; Roop, R.; Monk, D.J.; Almanza-Workman, A.M.; Raghavan, S. Water dispersible silanes for wettability modification of polysilicon. *J. Electrochem. Soc.* **2002**, *149*, H6–H11.
97. Takatani, Y.; Yamakawa, K.; Yoshizawa, S. Corrosion behaviour of aluminum alloys in saturated calcium hydroxide solution. *Zair. Soc. Mater. Sci. Jpn.* **1983**, *32*, 1218–1222. [[CrossRef](#)]
98. Yamamoto, S.; Sugiyama, S.; Matsuoka, O.; Kohmura, K.; Honda, T.; Banno, Y.; Nozoye, H. Dissolution of zeolite in acidic and alkaline aqueous solutions as revealed by AFM imaging. *J. Phys. Chem.* **1996**, *100*, 18474–18482. [[CrossRef](#)]
99. Kumaraguru, S.P.; Veeraraghavan, B.; Popov, B.N. Development of an electroless method to deposit corrosion-resistant silicate layers on metallic substrates. *J. Electrochem. Soc.* **2006**, *153*, B253–B259. [[CrossRef](#)]
100. Deyá, C.; Romagnoli, R.; Del Amo, B. A new pigment for smart anticorrosive coatings. *J. Coat. Technol. Res.* **2007**, *4*, 167–175. [[CrossRef](#)]
101. Chico, B.; Simancas, J.; Vega, J.M.; Granizo, N.; Díaz, I.; de la Fuente, D.; Morcillo, M. Anticorrosive behaviour of alkyd paints formulated with ion-exchange pigments. *Prog. Org. Coat.* **2008**, *61*, 283–290. [[CrossRef](#)]
102. Zheng, Z.; Schenderlein, M.; Huang, X.; Brownbill, N.J.; Blanc, F.; Shchukin, D. Influence of functionalization of nanocontainers on self-healing anticorrosive coatings. *ACS Appl. Mater. Interfaces* **2015**, *7*, 22756–22766. [[CrossRef](#)]
103. Ghosh, S.K. *Functional Coatings: By Polymer Microencapsulation*; Wiley: Weinheim, Germany, 2006; ISBN 352731296X.
104. Samadzadeh, M.; Boura, S.H.; Peikari, M.; Kasiriha, S.M.; Ashrafi, A. A review on self-healing coatings based on micro/nanocapsules. *Prog. Org. Coat.* **2010**, *68*, 159–164. [[CrossRef](#)]
105. Stankiewicz, A.; Szczygieł, I.; Szczygieł, B. Self-healing coatings in anti-corrosion applications. *J. Mater. Sci.* **2013**, *48*, 8041–8051. [[CrossRef](#)]
106. Rivera-Garza, M.; Olguín, M.T.; García-Sosa, I.; Alcántara, D.; Rodríguez-Fuentes, G. Silver supported on natural Mexican zeolite as an antibacterial material. *Microporous Mesoporous Mater.* **2000**, *39*, 431–444. [[CrossRef](#)]
107. Kwakye-Awuah, B.; Williams, C.; Kenward, M.A.; Radecka, I. Antimicrobial action and efficiency of silver-loaded zeolite X. *J. Appl. Microbiol.* **2008**, *104*, 1516–1524. [[CrossRef](#)] [[PubMed](#)]

108. Ferreira, L.; Fonseca, A.M.; Botelho, G.; Aguiar, C.A.; Neves, I.C. Antimicrobial activity of faujasite zeolites doped with silver. *Microporous Mesoporous Mater.* **2012**, *160*, 126–132. [[CrossRef](#)]
109. McDonnell, A.M.P.; Beving, D.; Wang, A.; Chen, W.; Yan, Y. Hydrophilic and antimicrobial zeolite coatings for gravity-independent water separation. *Adv. Funct. Mater.* **2005**, *15*, 336–340. [[CrossRef](#)]
110. Chanda, R.; Selvam, T.; Herrmann, R.; Schwieger, W. Reactive coating process for binder-free zeolite FAU films on metallic aluminum supports. *Mater. Lett.* **2018**, *211*, 103–106. [[CrossRef](#)]
111. Calabrese, L.; Brancato, V.; Bonaccorsi, L.; Frazzica, A.; Capri, A.; Freni, A.; Proverbio, E. Development and characterization of silane-zeolite adsorbent coatings for adsorption heat pump applications. *Appl. Therm. Eng.* **2017**, *116*, 364–371. [[CrossRef](#)]
112. Aramaki, K. Preparation of protective films containing molybdate for self-healing of a scratched iron surface. *Corrosion* **2000**, *56*, 901–909. [[CrossRef](#)]
113. Lin, B.L.; Lu, J.T.; Kong, G. Effect of molybdate post-sealing on the corrosion resistance of zinc phosphate coatings on hot-dip galvanized steel. *Corros. Prot.* **2007**, *50*, 962–967. [[CrossRef](#)]
114. Trabelsi, W.; Cecilio, P.; Ferreira, M.G.S.; Montemor, M.F. Electrochemical assessment of the self-healing properties of Ce-doped silane solutions for the pre-treatment of galvanised steel substrates. *Prog. Org. Coat.* **2005**, *54*, 276–284. [[CrossRef](#)]
115. Schoonheydt, R.A.; Geerlings, P.; Pidko, E.A.; Van Santen, R.A. The framework basicity of zeolites. *J. Mater. Chem.* **2012**, *22*, 18705–18717. [[CrossRef](#)]
116. Song, Y.; Shan, D.; Chen, R.; Han, E.H. Corrosion characterization of Mg-8Li alloy in NaCl solution. *Corros. Sci.* **2009**, *51*, 1087–1094. [[CrossRef](#)]
117. Majdi, M.R.; Danaee, I.; Afghahi, S.S.S. Preparation and anti-corrosive properties of cerium oxide conversion coatings on steel X52. *Mat. Res.* **2017**, *20*, 445–451. [[CrossRef](#)]
118. Volarič, B.; Milošev, I. Rare earth chloride and nitrate salts as individual and mixed inhibitors for aluminium alloy 7075-T6 in chloride solution. *Corros. Eng. Sci. Technol.* **2017**, *52*, 201–211. [[CrossRef](#)]
119. Yan, W.; Ong, W.K.; Wu, L.Y.; Wijesinghe, S.L.; Yan, W.; Ong, W.K.; Wu, L.Y.; Wijesinghe, S.L. Investigation of using sol-gel technology for corrosion protection coating systems incorporating colours and inhibitors. *Coatings* **2019**, *9*, 52. [[CrossRef](#)]
120. Wang, T.; Du, J.; Ye, S.; Tan, L.; Fu, J. Triple-stimuli-responsive smart nanocontainers enhanced self-healing anticorrosion coatings for protection of aluminum alloy. *ACS Appl. Mater. Interfaces* **2019**, *11*, 4425–4438. [[CrossRef](#)] [[PubMed](#)]
121. Kanu, N.J.; Gupta, E.; Vates, U.K.; Singh, G.K. Self-healing composites: A state-of-the-art review. *Compos. A Appl. Sci. Manuf.* **2019**, *121*, 474–486. [[CrossRef](#)]
122. Den Brabander, M.; Fischer, H.R.; Garcia, S.J. Self-healing polymeric systems: Concepts and applications. In *Smart Polymers and their Applications*, 2nd ed.; Aguilar, M.R., Román, J.S., Eds.; Woodhead Publishing: Sawston, UK, 2019; pp. 379–409. ISBN 978-0-08-102416-4.
123. Samiee, R.; Ramezanzadeh, B.; Mahdavian, M.; Alibakhshi, E. Assessment of the smart self-healing corrosion protection properties of a water-base hybrid organo-silane film combined with non-toxic organic/inorganic environmentally friendly corrosion inhibitors on mild steel. *J. Clean. Prod.* **2019**, *220*, 340–356. [[CrossRef](#)]
124. Zhao, X.; Li, Y.; Li, B.; Hu, T.; Yang, Y.; Li, L.; Zhang, J. Environmentally benign and durable superhydrophobic coatings based on SiO<sub>2</sub> nanoparticles and silanes. *J. Colloid Interface Sci.* **2019**, *542*, 8–14. [[CrossRef](#)] [[PubMed](#)]
125. Liu, Y.; Gu, H.; Jia, Y.; Liu, J.; Zhang, H.; Wang, R.; Zhang, B.; Zhang, H.; Zhang, Q. Design and preparation of biomimetic polydimethylsiloxane (PDMS) films with superhydrophobic, self-healing and drag reduction properties via replication of shark skin and SI-ATRP. *Chem. Eng. J.* **2019**, *356*, 318–328. [[CrossRef](#)]
126. Lopez de Armentia, S.; Pantoja, M.; Abenojar, J.; Martinez, M.; Lopez de Armentia, S.; Pantoja, M.; Abenojar, J.; Martinez, M.A. Development of silane-based coatings with zirconia nanoparticles combining wetting, tribological, and aesthetical properties. *Coatings* **2018**, *8*, 368. [[CrossRef](#)]
127. Ma, L.; Svec, F.; Tan, T.; Lv, Y. In-situ growth of highly permeable zeolite imidazolate framework membranes on porous polymer substrate using metal chelated polyaniline as interface layer. *J. Membrane Sci.* **2019**, *576*, 1–8. [[CrossRef](#)]
128. Tan, Y.; Wang, F.; Zhang, J. Design and synthesis of multifunctional metal-organic zeolites. *Chem. Soc. Rev.* **2018**, *47*, 2130–2144. [[CrossRef](#)] [[PubMed](#)]

129. Wang, J.; Song, X.; Wang, J.; Cui, X.; Zhou, Q.; Qi, T.; Li, G.L. Smart-sensing polymer coatings with autonomously reporting corrosion dynamics of self-healing systems. *Adv. Mater. Interfaces* **2019**, *6*, 1900055. [[CrossRef](#)]
130. Karami, Z.; Maleki, S.; Moghaddam, A.; Jahandideh, A. Self-healing bio-composites: Concepts, developments, and perspective. In *Sustainable Polymer Composites and Nanocomposites*; Springer: Cham, Switzerland, 2019; pp. 1323–1343.
131. Catauro, M.; Vecchio Cipriotti, S. Sol-gel synthesis and characterization of hybrid materials for biomedical applications. In *Thermodynamics and Biophysics of Biomedical Nanosystems*; Demetzos, C., Pippa, N., Eds.; Springer: Singapore, 2019; pp. 445–475.



© 2019 by the authors. Licensee MDPI, Basel, Switzerland. This article is an open access article distributed under the terms and conditions of the Creative Commons Attribution (CC BY) license (<http://creativecommons.org/licenses/by/4.0/>).